LUNG STRUCTURE-RESPIRATORY FUNCTION RELATIONSHIPS IN EXPERIMENTALLY-INDUCED BRONCHIOLITIS, BRONCHOPNEUMONIA AND INTERSTITIAL PNEUMONIA IN RATS

PRINCIPAL INVESTIGATORS
J. L. Mauderly
E. de Madron
J. R. Harkema

Abstract — Histopathology and respiratory function of rats with three different types and distributions of lower lung inflammation were compared to better understand lung structure-function relationships. Rats were exposed 21 h/day for 7 days to 0.8 ppm ozone (O_3), sham-exposed as controls, or given 5 mg/kg bacterial endotoxin either intratracheally (ITE) or intraperitoneally (IPE). Respiratory function was measured 24 h after the end of treatment, then the rats were sacrificed and the distribution of inflammation was evaluated morphometrically. Chronic centriacinar inflammation with formation of new respiratory bronchioles caused an obstructive functional impairment in the O_3 rats, which was clearly distinguished from the restrictive impairments resulting from acute inflammation in ITE and IPE rats. Only the magnitudes of changes related to the distribution of inflammation differentiated the ITE and IPE groups. Flow parameters previously thought sensitive to large airway resistance were changed in the O_3 rats. Alveolar luminal inflammatory exudate affected quasistatic compliance more than septal inflammation in ITE and IPE rats. Quasistatic chord compliance was the most sensitive of three indices of pressure-volume relationships. The findings in this study improve the basis for interpreting respiratory function changes of rats.

Respiratory function data reveal the functional impact of lung pathology, and are widely used in human medicine and epidemiological and clinical studies of inhaled toxicants. Most tests have been adapted for animals and are important adjuncts to inhalation toxicological studies.[1] Functional parameters are integrative by nature, and can be similarly affected by different types of lesions. Although these tests can detect functional abnormalities with good sensitivity and can distinguish among different physiological types of impairment, their ability to distinguish among morphological lesions of different types and distributions is limited.

There is considerable information on general lung structure-function relationships in rats with different lung diseases, but the diseases typically consisted of lesions of mixed types and distribution. In addition, most of the diseases examined involved chronic lesions. The present study was conducted to better understand lung structure-function relationships in rats with deep lung inflammation of three different types and distributions. The lesions included ozone-induced bronchiolitis (subchronic inflammation confined to centriacinar region), endotoxin-induced bronchopneumonia (acute inflammation involving small airways and alveolar parenchyma), and endotoxin-induced interstitial pneumonia (limited to alveolar septa). The goals were to probe the sensitivities of the function tests to these lesions and to test hypotheses about the impacts of small airway and parenchymal lesions on respiratory function of rats.

METHODS

Forty female F344/N rats, 14-18 wk of age, were assigned to four treatment groups of 10 animals each: sham-exposed control (C), ozone (O_3), intratracheal endotoxin (ITE), and intraperitoneal endotoxin (IPE). The C and O_3 groups were acclimated to inhalation exposure

chambers for 1 wk before ozone or sham exposures began. The O_3 group was then exposed to 0.83 ± 0.01 ppm of ozone for 21.4 ± 1.7 h/day, for 7 days. The C rats were sham-exposed to clean air.

The ITE and IPE groups were maintained in colony housing. The ITE group was instilled intratracheally with approximately 5 mg/kg of endotoxin (lipopolysaccharide from Escherichia Coli O111:B4, Sigma Chemical, St. Louis, MO) in 0.2 mL of a 5 mg/mL solution in pyrogen-free saline. The IPE group was injected intraperitoneally with approximately 5 mg/kg of endotoxin in saline at a total volume of 1.0 mL.

Baseline respiratory function was measured before treatment. The C and O_3 groups were retested immediately after the end of the 7-day sham or ozone exposure. The ITE and IPE groups were retested at 24 h after treatment. Anesthetized rats were tested by plethysmography as described previously.[1,2] Breathing patterns, dynamic lung compliance (Cdyn) and total pulmonary resistance (R_L) were measured during spontaneous respiration. Other parameters were measured during single-breath maneuvers induced by positive and negative airway pressures. All physiological lung volumes were measured, including total lung capacity (TLC), vital capacity (VC), functional residual capacity (FRC), and residual volume (RV). Pressure-volume (P-V) relationships were evaluated by measuring the quasistatic chord compliance (Cqc) of the P-V curve between -2 and +4 cm H_2O transpulmonary pressure (Ptp); the maximum quasistatic compliance (Cqm) was measured over a 2 cm H_2O Ptp segment of the P-V curve; and, a P-V curve shape factor (D) was derived by curve fitting.[3] The homogeneity of gas distribution in the lung was evaluated by measuring the slope of phase III of the single-breath N_2 washout (SIII). Alveolar-capillary gas exchange was evaluated by measuring the single-breath CO diffusing capacity (D_{LCO}). Forced expiratory parameters used to assess flow limitation included the percentage of forced vital capacity (FVC) exhaled in 0.1 sec ($FEV_{.1}$%), peak expiratory flow (PEFR), mean mid-expiratory flow (MMEF) over 25-75% of FVC, maximal expiratory flow at 50%, 35%, and 10% of FVC (MEF_{50}, MEF_{35}, MEF_{10}), and the upstream flow resistance at 35% FVC (Rus_{35}).

Immediately after post-treatment function tests, the rats were euthanized and the heart-lung block was excised. Lungs were fixed in 10% neutral buffered formalin for 24 h at a tracheal pressure of 25 cm, and the external volume of the lungs was measured by water displacement. Six to eight 1 mm thick sagittal sections of the left lung were cut, embedded, sectioned at 5 μm, and stained with hematoxylin-eosin.

Morphometry was done in 2 stages. The distribution and extent of inflammation was quantitated by examining airways, centriacinar regions, and parenchyma at 400x. Airways were restricted to circular airway cross-sections that did not have alveolar outpockets. Centriacinar regions were defined as areas centered on the junction between terminal airways and alveolar ducts, and having a three-cell radius (approximately 50 μm). Parenchymal regions contained only alveoli and small blood vessels.

All airways on the slides were examined. Airways having 10 or more neutrophils in their walls were considered inflamed (bronchitis or bronchiolitis). All centriacinar regions were examined. Those regions having 10 or more neutrophils in terminal bronchioles or alveolar septa were considered acutely inflamed. Regions with epithelial hyperplasia, interstitial fibrosis, and macrophages in the airspaces were considered chronically inflamed. Five random parenchymal fields per slide were evaluated. Inflammation was considered to be present in each field when 10 or more neutrophils were present in alveolar septa or in alveolar lumens. In all regions, fields not meeting the criteria for inflammation were considered normal. The results were expressed as percentages of normal, acutely inflamed, or chronically inflamed fields. Parenchymal inflammation was further described as the percentage of inflamed fields containing either septal or luminal inflammation.

The portion of lung volume occupied by different structures was also determined. A 58-point square-lattice grid was optically superimposed on 100x microscopic images and the number of points falling on each structure was counted. Eight structures were examined: alveolar septum and lumen, respiratory bronchiolar wall and lumen, airway (bronchiolar/bronchial) wall and lumen, blood vessels (wall + lumen), and peribronchiolar/perivascular interstitium. The volume of each structure and the percentage of lung volume occupied by each structure were estimated using standard equations.

The significance of treatment effects on respiratory function was determined using paired t tests of baseline and post-treatment respiratory function data. The percentage change from baseline was calculated for each rat and the magnitudes of percentage changes were compared among groups. Group differences in post-treatment morphometric data were evaluated by multiple comparisons using pairwise t tests with the Bonferroni adjustment for multiple contrasts. The criterion for statistical significance was set at $p < 0.05$.

RESULTS

All baseline respiratory function values fell within normal ranges. No inflammation was detected in the lungs of the C group (Table 1). The only significant changes in respiratory function of the C group were increases in Cdyn, and Cqc (Table 2).

Ninety-three percent of the centriacinar fields from the O_3 group had chronic inflammation of the centriacinar fields, which included Type II epithelial cell hyperplasia and clusters of macrophages in the adjacent airspaces, fibrosis of terminal bronchiolar and alveolar duct walls and interstitium of proximal alveolar septa, and remodeling resulting in the formation of new respiratory bronchioles, and thickening of adjacent alveolar septa (Table 1). There was little

Table 1

Distribution of Inflammation, as Percentage of Microscopic Fields Observed

(n = 10/Group)

	Control (C)		Ozone (O_3)		II Endotoxin (IIE)		IP Endotoxin (IPE)	
Structure	$\bar{X}$	SE	$\bar{X}$	SE	$\bar{X}$	SE	$\bar{X}$	SE
Airways								
Normal	100	0	99	1	14	2	99	1
Inflamed	0	0	1	1	86	2	1	1
Centriacinar Region								
Normal	100	0	7	1	76	3	100	0
Acutely Inflamed	0	0	0	0	24	3	0	0
Chronically Inflamed	0	0	93	1	0	0	0	0
Parenchyma (Alveoli)								
Normal	100	0	100	0	33	6	66	4
Inflamed	0	0	0	0	67	6	34	4
% Septal[a]	0	0	0	0	21	3	99	1
% Luminal[a]	0	0	0	0	100	0	2	1

[a]Percentage of inflamed fields containing septal or luminal inflammation.

Table 2

Percentage Baseline to Post-Treatment Changes in Breathing Pattern, Lung Compliance, Intrapulmonary Gas Distribution, and Alveolar-Capillary Gas Exchange

(n = 10/Group)

		Control (C)		Ozone (O_3)		IT Endotoxin (ITE)		IP Endotoxin (IPE)	
Variable	Definition	$\bar{X}$	SE	$\bar{X}$	SE	$\bar{X}$	SE	$\bar{X}$	SE
f	Respiratory Frequency	4[a]	1	2	2	-1	3	-1	1
V_T	Tidal Volume	21	10	-33[a]	6	-28[a]	5	-16[a]	6
$\dot{V}_E$	Minute Volume	18	8	-30[a]	6	-32[a]	5	-16	9
Cdyn	Dynamic Compliance	-12[a]	5	-21[a]	8	15[a]	6	7	9
Cqc	Quasistatic Chord Compliance	25[a]	10	-13	8	-43[a]	5	-26[a]	8
Cqm	Max. Quasistatic Compliance	4	9	-9	13	-43	5	-14	9
D	P-V Cure Shape Factor	15	-[b]	-9	-	-40[a]	--	-19	--
TLC	Total Lung Capacity	-3	3	-3	4	-15[a]	1	-9[a]	2
VC	Vital Capacity	-3	3	-13[a]	2	-19[a]	2	-12[a]	2
VC/TLC		-1	2	-10[a]	2	-4	2	-3	2
FRC	Functional Residual Capacity	-7	8	79[a]	16	26[a]	6	18	12
FRC/TLC		-5	6	83[a]	12	48[a]	4	28[a]	11
RV	Residual Volume	0	24	118[a]	35	21	20	12	18
RV/TLC		10	27	119[a]	28	43	20	22	19
SIII	Slope Phase III N_2 Washout	1	6	67[a]	18	46[a]	12	29[a]	13
D_{LCO}	CO Diffusing Capacity	-3	5	-18	9	-33[a]	3	-15	8
D_L/V_A	D_{LCO}/Alveolar Volume	-8	6	-19[a]	8	-31[a]	4	-2	10

[a]Difference from baseline significant at $p < 0.05$.

[b]Curve fitting produced SE for baseline and post-treatment group means, but not for percentage differences.

inflammation in more proximal small airways (only 1% of fields) and no inflammation in fields containing only distal alveoli. Centriacinar remodeling was reflected by marked increases in the respiratory bronchiolar wall and luminal volumes (Table 3); respiratory bronchioles were rarely found in lungs of the other three groups. Effects in adjacent structures were reflected by increases in airway wall and luminal volumes, an increased alveolar septal volume, and a decrease in alveolar luminal volume.

Ozone caused a primarily obstructive functional impairment with gas mixing and gas exchange abnormalities. The R_L was more than doubled (Table 4). Forced expiratory flow was reduced at all lung volumes, with significant reductions in PEFR and MMEF. Although Rus_{35} was doubled, high variability prevented the change from reaching statistical significance. Ozone reduced both VC and FVC by increasing RV (Table 2). There was little reduction of TLC, as can be seen in the P-V curve (Fig. 1). The FRC was also increased (Table 2). The Cdyn was significantly reduced. All indices of quasistatic compliance were slightly, but not significantly, reduced. An inhomogeneity of gas distribution was indicated by an increased SIII. Alveolar-capillary gas exchange efficiency was slightly reduced, but the effect was significant only for D_L/V_A.

Intratracheal endotoxin resulted in acute bronchopneumonia characterized by acute inflammation with a locally extensive (or widespread) distribution, including 86% of airways, 24% of

Table 3

Portions of Left Lung Volume Occupied by Individual Structures

(n = 10/Group)

Structure	Units	Control (C) $\bar{X}$	Control (C) SE	Ozone (O_3) $\bar{X}$	Ozone (O_3) SE	IT Endotoxin (ITE) $\bar{X}$	IT Endotoxin (ITE) SE	IP Endotoxin (IPE) $\bar{X}$	IP Endotoxin (IPE) SE
Left Lung Volume	mL	2.5	0.1	2.8	0.1	2.3	0.1	2.1[a]	0.1
Small Airway Wall	mm^3	21.5	3.5	45.1[a]	5.4	30.6	4.7	27.1	2.7
	(%)	(0.8	0.1)	(1.6[a]	0.2)	(1.4	0.2)	(1.3	0.2)
Small Airway Lumen	mm^3	74.9	20.3	189.5[a]	29.2	158.9[a]	13.7	132.6	19.8
	(%)	(2.9	0.8)	(6.6[a]	0.9)	(6.9[a]	0.6)	(6.3[a]	1.0)
Blood Vessels	mm^3	62.6	10.1	85.2	10.2	90.9	9.4	68.7	9.3
	(%)	(2.5	0.4)	(3.0	0.3)	(4.0[a]	0.4)	(3.3	0.4)
Peribronchial/Perivascular	mm^3	37.2	7.5	72.6[a]	11.5	117.4[a]	11.0	40.1	5.7
	(%)	(1.5	0.3)	(2.7	0.4)	(5.2[a]	0.6)	(1.9	0.3)
Respiratory Bronchiole Wall	mm^3	0.7	0.5	10.4[a]	1.7	0.5	0.2	0.7	0.3
	(%)	(0.002	0.002)	(0.37[a]	0.05)	(0.02	0.01)	(0.03	0.01)
Respiratory Bronchiole Lumen	mm^3	1.0	0.4	40.1[a]	7.0	3.6	1.5	1.5	0.7
	(%)	(0.04	0.02)	(1.43[a]	0.24)	(0.18	0.09)	(0.07	0.04)
Alveolar Septum	mL	0.38	0.01	0.48[a]	0.03	0.46[a]	0.03	0.41	0.02
	(%)	(14.9	0.5)	(17.0[a]	0.7)	(19.8[a]	0.5)	(19.3[a]	0.6)
Alveolar Lumen	mL	1.97	0.07	1.90	0.11	1.45[a]	0.08	1.45[a]	0.11
	(%)	(77.4	1.6)	(67.2[a]	1.4)	(62.4[a]	1.6)	(67.6	1.2)

[a]Difference from control significant at $p < 0.05$ by multiple comparison and Bonferroni adjustment for 3 contrasts.

Table 4

Percentage Baseline to Post-Treatment Changes in Flow-Conducting Properties of Airways

(n = 10/Group)

Variable	Definition	Control (C) $\bar{X}$	Control (C) SE	Ozone (O_3) $\bar{X}$	Ozone (O_3) SE	IT Endotoxin (ITE) $\bar{X}$	IT Endotoxin (ITE) SE	IP Endotoxin (IPE) $\bar{X}$	IP Endotoxin (IPE) SE
R_L	Total Pulmonary Resistance	8	11	165[a]	57	28	22	-8	14
FVC	Forced Vital Capacity	-5	3	-19[a]	3	-15[a]	2	-8[a]	2
$FEV_{.1}$%	% FVC Exhaled in 0.1 Sec	-5	6	-3	5	20[a]	5	14[a]	6
PEFR	Peak Exp. Flow	-9	7	-20[a]	8	2	4	2	4
MMEF	Mean Midexpiratory Flow	-7	12	-24[a]	1	16	11	16	11
MEF_{50}	Max. Exp. Flow at 50% FVC	-10	13	-19	9	14	11	18	13
MEF_{35}	Max. Exp. Flow at 35% FVC	-1	15	-21	7	51	25	39[a]	15
MEF_{10}	Max. Exp. Flow at 10% FVC	-10	14	-10	18	-2	17	7	17
Rus_{35}	Upstream Resist. at 35% FVC	64	51	112	59	-28	17	-21	19

[a]Difference from baseline significant at $p < 0.05$.

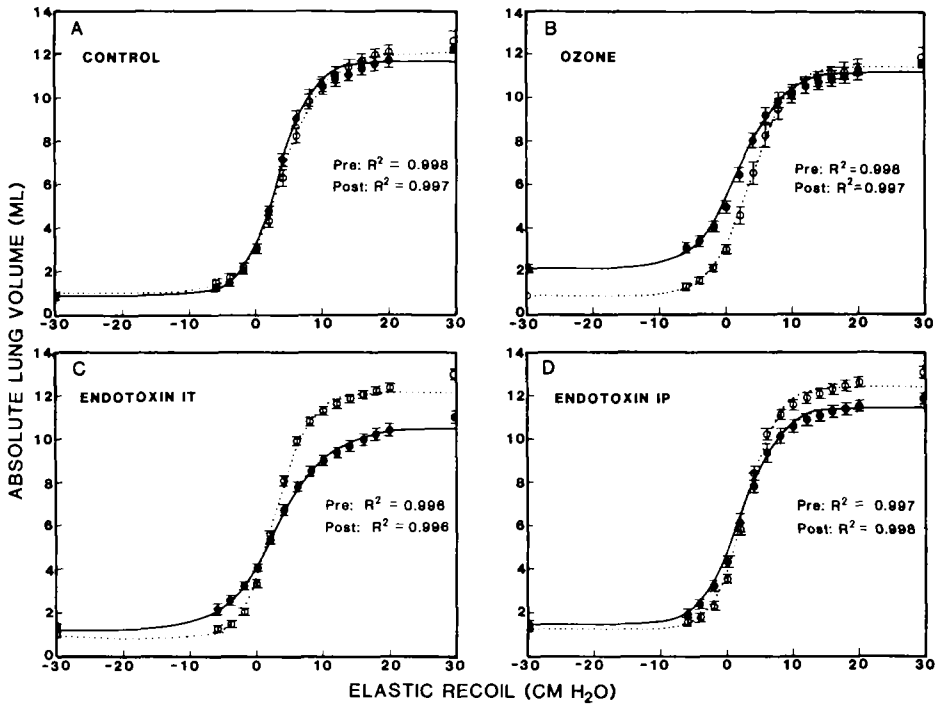

Figure 1. Curves fit to quasistatic pressure-volume data by equation of Pavia et al.[3] Open circles = baseline, closed circles = post-treatment (mean ± SE, n = 10). The squares of the coefficients of correlation (R^2) given for each curve indicate an excellent fit to the data. Values for the shape parameter, D, are given in Table 3. These curves illustrate the effects of treatment on both compliance (slope) and on minimal (RV) and maximal (TLC) lung volumes.

centriacinar fields, and 67% of alveolar fields (Table 1). This acute inflammation, which was centered around both upper and lower intrapulmonary airways, was characterized by a massive influx of neutrophils along with accumulation of fibrinous material in septa and airspaces, and was therefore acute, rather than chronic as in the O_3 group. All inflamed parenchymal fields had increased neutrophils in alveolar lumens, while septa were inflamed in only 21% of the inflamed fields. The inflammation in airways increased the airway wall volume only slightly, but significantly increased the volume of small airway lumens (Table 3). The widespread acute inflammation caused a slight increase in blood vessel volume and a significant increase in peribronchial/perivascular interstitial volume. The alveolar inflammation was reflected by an increase in septal volume and a decrease in luminal volume.

The IIE group had a restrictive functional impairment with gas distribution and gas exchange abnormalities, but no airflow obstruction. The rats had labored breathing and were difficult to stabilize for the tests. The treatment reduced TLC and VC, and increased FRC and RV (Table 2). All indices of quasistatic compliance were decreased (significant for Cqc and D), and the slope of the P-V curve (Fig. 1) was clearly reduced. In contrast, Cdyn was increased (Table 2). An inhomogeneity of gas distribution was reflected by a increased SIII, and impaired alveolar-capillary gas exchange was reflected by a reduced D_{LCO}. Because both D_{LCO} and D_L/V_A were reduced similarly, the gas exchange impairment was not due to the reduced lung volume. Forced expiratory flows were slightly increased, except for a slight decrease of MEF_{10}, and Rus_{35} was slightly decreased (Table 4). The reduction of FVC and increased flows caused $FEV_{.1}$% to be significantly increased (Table 4). Paradoxically, there was a slight increase in R_L (Table 2).

The IPE rats had a patchy interstitial pneumonia in deep lung parenchyma with no inflammation in airways or the centriacinar region (Table 1). Although alveolar parenchyma was the only region

affected, only 34% of the alveolar fields were inflamed. The inflammation involved primarily alveolar septal interstitium (99% of inflamed fields); the alveolar lumen was involved in only 2% of the inflamed fields. Alveolar septal volume was increased and alveolar luminal volume was decreased (Table 3). Small airway luminal volume was slightly increased.

The interstitial pneumonia caused a restrictive functional defect with gas distribution and gas exchange abnormalities, but no airflow obstruction. It was also difficult to stabilize this group for the tests, although not as difficult as for the ITE group. The TLC and VC were reduced (Table 2), primarily by limiting maximal lung expansion (Fig. 1), while FRC and RV were slightly increased (Table 2). All indices of quasistatic compliance were reduced, but only the effect on Cqc was significant. In contrast, Cdyn was slightly increased. The SIII was increased and DL_{CO} was slightly decreased. There was no airflow limitation; the resistances to both tidal (R_L) and forced (Rus_{35}) airflow were actually reduced (Table 4). Forced expiratory flows were slightly increased throughout the exhalation. The reduced FVC and increased flows caused a significant increase of $FEV_{.1}$%.

DISCUSSION

Few of the functional parameters distinguished clearly among these three models of deep lung inflammation. All treatments caused reductions of quasistatic compliance, VC, and D_{LCO}, and increases of FRC, RV, and SIII; however, the magnitudes of these changes differed among the groups. Forced expiratory parameters clearly distinguished the O_3 group from the ITE and IPE groups. Although FVC was reduced in all groups, forced flows and $FEV_{.1}$% were decreased in O_3 and increased in ITE and IPE. The changes in Rus_{35} were also opposite in the ozone and endotoxin-treated groups, and R_L was significantly increased only in the O_3 group. No functional parameters clearly distinguished between the ITE and IPE groups. The primary differences between these groups were the greater magnitudes of change in TLC, quasistatic compliance, RV, SIII, and D_{LCO} in the ITE rats.

The effects of ozone on airflow parameters suggest that the site-specificity of these parameters might differ between man and rats. The centriacinar lesions caused increased resistance to flow throughout the lung volume range and during both forced and tidal breathing. In man, flow limitation at high lung volumes is thought to be more sensitive to alterations in large airways, while flow limitation at low volumes is thought to be more sensitive to alterations in small airways.[4] In addition, R_L during tidal breathing is thought to largely reflect flow resistance in upper airways of man, and has been shown to be relatively insensitive to experimental lower airway blockage in the dog.[5] The R_L of the O_3 rats was increased in the absence of significant changes in upper airways, and the magnitude of the increase in R_L was greater than that of Rus_{35}, a parameter theoretically reflecting peripheral airway resistance.[4] Forced flow limitation at all lung volumes, and increases in Rus_{35} and R_L have also been observed in rats with acrolein-induced lesions in lower airways and parenchyma.[6] These findings indicate that R_L and forced flows at high lung volumes are sensitive to changes in small airways of rats, and suggest the need for more detailed studies of interspecies differences in the sites and mechanisms of flow limitation.

Forced flows of the ITE and IPE groups were increased and Rus_{35} was decreased. An increased radial traction on small airways due to the increased elastic recoil of the alveolar parenchyma, in the absence of substantial airway disease, probably caused this effect.[7] In a previous study,[8] an increased elastic recoil due to focal inflammation and fibrosis was thought to have prevented flow limitation from focal emphysema in rats with mixed lesions induced by chronic diesel exhaust inhalation. The present results, however, indicate that flow can actually be greater than normal in lungs with a stiffened parenchyma, but without significant airway lesions.

The data collected during spontaneous respiration in this study suggest that these variables may have little interpretive value in rats with acute inflammatory lesions that render them dyspneic and difficult to stabilize under anesthesia. The O_3 rats presented no particular difficulty, and their reduced Cdyn and increased R_L are consistent with results of single-breath tests measured under more controlled conditions. The increased Cdyn in the ITE and IPE groups was not consistent with their reduced quasistatic compliance, including Cqc, which is measured in the tidal portion of the P-V curve.

All three treatments reduced VC (and FVC) and compliance; however, ozone reduced VC primarily by increasing RV, while both IT and IP endotoxin increased VC predominantly by changes in TLC. The increases in RV in all treated groups were probably due to small airway closure earlier during exhalation, since the increase in parenchymal tissue volume and decrease in alveolar airspace volume would have acted to reduce RV. The finding of the greatest change in RV in the group (O_3) with the most focally located and chronic centriacinar inflammatory response, suggests that in lower lung inflammation in the rat, RV is most sensitive to changes in the centriacinar region.

The TLC of both the ITE and IPE groups was reduced by limitation of maximal lung expansion, and the greater reduction in the ITE group was consistent with that group's greater reduction of quasistatic compliance. Although quasistatic compliance has been thought to primarily reflect the stiffness of alveolar septa,[1] this study demonstrated that luminal inflammatory exudate is also an important factor. Septal inflammation was present in only 14% of the parenchymal fields in the ITE group (67% inflamed x 21% septal); thus, the inflammation observed in 24% of the centriacinar fields and luminal inflammation observed in 67% of the parenchymal fields reduced quasistatic compliance more than the septal inflammation observed in 34% of the parenchymal fields in the IPE group.

There was little difference in the descriptive ability of the three indices of quasistatic compliance, Cqc, Cqm, and D; all changed in parallel. The magnitude of change of Cqc of all groups was greater than that of D, and equal to or greater than that of Cqm. If any of the three parameters offered an advantage in sensitivity, therefore, it was Cqc. This parameter is the slope of the curve over a 6 cm H_2O chord in the tidal breathing range. The Cqm reflected the P-V relationship over the smallest chord of the curve, 2 cm H_2O, and might be expected to be the least representative of changes in overall curve shape. The equation used to fit the P-V curves and to calculate D resulted in excellent curve fits; therefore, D should have been an accurate reflection of the shape of the entire curve. The finding that Cqc was more sensitive than D to the reduced compliance is in agreement with the report that quasistatic chord compliance was more sensitive than the curve shape factor to increases in compliance of rat lungs resulting from enzyme-induced emphysema and cigarette smoke exposure.[9]

The FRC was increased by all treatments. The results of this study and others indicate that the relaxed, end-expiratory volume ("FRC") of the anesthetized rat cannot be interpreted in the same manner as the FRC of man. The FRC of rats has been shown to increase in chronic lung disorders of diverse types that both increase and decrease lung elastic recoil.[1] In species such as man and dog, with stiff chest walls, the FRC is predominantly set by the balance between outward recoil of the chest wall and inward elastic recoil of the lung.[10] In the rat, with a highly compliant chest wall, the relaxed lung volume of anesthetized subjects is smaller than the end-expiratory lung volume of the conscious subject,[10] which is set by mechanisms other than the balance of compliances. It appears likely that lung tissue changes of diverse types tend to "fix" the relaxed lung volume of the rat close to the conscious FRC and that, in the absence of substantial influence from the chest wall, this increases the anesthetized, relaxed lung volume. It would be useful (although difficult) to compare the effects of different lung disorders on the FRCs of conscious and anesthetized rats.

It appears that SIII is a useful, but nonspecific, indicator of the homogeneity of gas distribution in rats, and that it has structural correlates similar to those in man. All three treatments increased SIII, and the ranking suggests that centriacinar changes predominated the effect (greatest in O_3), rather than changes in elastic recoil (greatest in ITE), or the uniformity of distribution of inflammation (affecting the lowest percentage of fields in IPE). This observation is consistent with reports that increases in SIII in human lungs correlate better with small airway lesions than with loss of elastic recoil or alveolar lesions.[11]

It appears that D_{LCO} is a useful, but nonspecific, indicator of alveolar-capillary gas exchange efficiency in both rats and man. All treatments reduced gas exchange efficiency (reduced D_{LCO}), but the effect was significant only for the ITE group. This suggests that, as might be expected, the impairment was predominantly related to the extent of alveolar involvement.

In summary, the results of this study indicate that current respiratory function assays for rats can distinguish between lower lung inflammation causing primarily obstructive effects from that causing primarily restrictive effects, but have little ability to distinguish between parenchymal inflammatory processes causing restrictive effects and having only subtle differences in distributions. Although this finding is not surprising, the study did provide substantially more detailed information than previously available on the functional manifestations of small airway and alveolar disease in the rat, and pointed toward specific areas for additional study.

REFERENCES

1. Mauderly, J. L. Effect of Inhaled Toxicants on Pulmonary Function, in Concepts in Inhalation Toxicology (R. O. McClellan and R. F. Henderson, eds.), Hemisphere, Washington, DC, pp. 349-404, 1989.

2. Harkema, J. R., J. L. Mauderly, and F. F. Hahn. The Effects of Emphysema on Oxygen Toxicity in Rats, Am. Rev. Respir. Dis. 126: 1058-1065, 1982.

3. Pavia, M., J. C. Yernault, P. Van Eerdeweghe, and M. Englert. Sigmoid Model of Static Volume-Pressure Curve of Human Lung, Respir. Physiol. 23: 317-323, 1975.

4. Hyatt, R. E. Forced Expiration, in The Respiratory System, Handbook of Physiology (P. T. Macklem and J. Mead, eds.), Section 3, American Physiological Society, Bethesda, MD, pp. 295-314, 1986.

5. Brown, R., A. J. Woolcock, N. J. Vincent, and P. T. Macklem. Physiological Effects of Experimental Airway Obstruction with Beads, J. Appl. Physiol. 27: 328-335, 1969.

6. Costa, D. L., R. S. Kutzman, J. R. Lehman, and R. T. Drew. Altered Lung Function and Structure in the Rat After Subchronic Exposure to Acrolein, Am. Rev. Respir. Dis. 133: 286-291, 1986.

7. Mead, J., J. M. Turner, P. T. Macklem, and J. B. Little. Significance of the Relationship Between Lung Recoil and Maximum Expiratory Flow, J. Appl. Physiol. 22: 95-108, 1967.

8. Mauderly, J. L., N. A. Gillett, R. F. Henderson, R. K. Jones, and R. O. McClellan. Relationships of Lung Structural and Functional Changes to Accumulation of Diesel Exhaust Particles, Ann. Occup. Hyg., in press.

9. Lai, Y. L. and L. Diamond. Comparison of Five Methods of Analyzing Respiratory Pressure-Volume Curves, Respir. Physiol. 66: 147-155, 1986.

10. Gillespie, J. R. Mechanisms That Determine Functional Residual Capacity in Different Mammalian Species, Am. Rev. Respir. Dis. 128: S74-S77, 1983.

11. Berend, N. The Correlation of Lung Structure With Function, Lung 160: 115-130, 1982.